

Effects of solar variability on planetary plasma environments and habitability

César Bertucci

Instituto de Astronomía y Física del Espacio, Buenos Aires, Argentina
email: cbertucci@iafe.uba.ar

Abstract. Intrinsic and induced planetary magnetospheres are the result of the transfer of energy and linear momentum between the solar wind and, respectively, the magnetic field and the atmospheres of solar system bodies. This transfer seems to be, however, more critical to the atmospheric evolution of unmagnetized objects such as Mars and Venus, as locally ionized planetary particles are accelerated by solar-wind induced electric fields, leading to atmospheric escape. The nature of the obstacle to the solar wind being different, intrinsic and induced magnetospheres respond differently to solar cycle changes in solar photon flux and solar wind properties. The influence of solar variability on planetary magnetospheres and its implications for atmospheric evolution based upon remote and in situ spacecraft measurements, and numerical simulations are discussed. In particular, the case of unmagnetized objects where non-thermal escape process might have played a role in their habitability conditions is considered.

Keywords. solar activity, solar neighborhood, planets: habitability

1. Introduction

The Sun interacts with planets and other solar system bodies through radiation and plasma processes with important consequences on the evolution of their atmospheres. The solar system is permeated by the solar wind, the coronal plasma in supersonic expansion which carries the frozen-in interplanetary magnetic field. Several types of obstacles are formed as a result of the interaction of the solar wind flow with planetary objects, depending on whether these objects are magnetized or not magnetized. Magnetized planets like Earth ($M \approx 7.9 \times 10^{25} \text{ G cm}^3$), Saturn ($M \approx 4.6 \times 10^{28} \text{ G cm}^3$) or Jupiter ($M \approx 1.53 \times 10^{30} \text{ G cm}^3$) generate 'intrinsic magnetospheres' - cavities free from solar wind plasma whose outer boundary, the magnetopause, is located well above the planet's atmosphere. This prevents the direct interaction of the solar wind with their atmospheres.

The absence of strong intrinsic fields at Venus ($M < 3 \times 10^{21} \text{ G cm}^3$, Russell *et al.* 1980) and Mars ($M < 2 \times 10^{21} \text{ G cm}^3$, Acuña *et al.* 1998) results in the direct transfer of energy and momentum from the solar wind and the Interplanetary Magnetic Field (IMF) into the atmospheric ionized particles. This is also the case of Saturn's major moon, Titan ($M < 2 \times 10^{21} \text{ G cm}^3$, Ness *et al.* 1982), which interacts most of the time with the co-rotating plasma of Saturn's magnetosphere. In these three cases, a well-defined region of perturbed IMF and populated by solar wind and local plasma is formed. This region is referred to as 'induced magnetosphere' (see, e.g., Bertucci *et al.* 2011).

When the supersonic solar wind approaches the ionized atmosphere of an unmagnetized planet, the transfer of linear momentum and energy from the solar flow to the planetary charged particles occur both abruptly and gradually in plasma boundaries and regions, respectively. According to the magnetohydrodynamic (MHD) theory, two boundaries characterize the interaction: the bow shock (BS), where the flow becomes subsonic,

compressed and heated, and the so-called 'ionopause' (IP), a pressure balance boundary that encircles a region inaccessible to the solar wind plasma. Accordingly, MHD theory predicts -in the subsolar direction- a gradual build up of the magnetic pressure in the detriment of the initially dominant (just inside the shock) thermal pressure between the BS and the IP. The difference in the speed of the plasma between the subsolar region and the flanks results in the draping of IMF field lines around the body and the formation of an 'induced' magnetotail consisting of two magnetic lobes with field lines parallel and anti-parallel to the incoming flow. In situ plasma measurements revealed the presence of an additional boundary located between the BS and IP, the induced magnetosphere boundary (IMB). The IMB is the outer boundary of the so called 'induced magnetosphere' and is characterized, among other signatures, by an abrupt increase in the magnetic field draping (Bertucci *et al.* 2003a,b) and the change in the dominant ion population, as solar wind ions start to be outnumbered by planetary ions (e.g., Dubinin *et al.* 2006, Martinecz *et al.* 2008, Bertucci *et al.* 2011). The occurrence of the IMB is associated with the role of the exosphere (in addition to the ionosphere) in the interaction as it is the source of locally ionized planetary ions above the ionosphere which are massively incorporated into the solar wind, reducing its momentum. This process, called massloading (Szego *et al.* 2000) is central in the interaction of the solar wind with active comets and involves the acceleration of local plasma via macroscopic (e.g. convective) and microscopic (e.g. electromagnetic waves) electric fields resulting from the drift between the solar wind and the planetary population in the context of the absence of collisions.

It is precisely inside the IMB that most of the escaping flux of atmospheric ions occurs (e.g., Fedorov *et al.* 2008) as a result of the action of a variety of acceleration processes taking place (Dubinin *et al.* 2011). In some cases, the escape of planetary ions stoichiometrically corresponds to the loss of water (e.g., Lundin *et al.* 2009), suggesting the link between the plasma escape problem and the evidence of dramatic changes in global climate and habitability conditions.

As a result, a better understanding of the nature and efficiency of the processes occurring within induced magnetospheres as well as their structure and variability in response to changes in the interplanetary plasma conditions are important to assess the evolution of the atmospheres of these objects. In this context, current investigations aim at answering the following questions: How much of the atmospheric evolution is caused by solar wind interactions? What is the effect of solar variability on these interactions and resulting atmospheric escape? What lessons can be learned for planets around other stars?

In this work we will not provide answers to them in detail, and we will only cover a few results obtained around planets Venus and Mars. In spite of these limitations, however, the results presented are key elements to build those answers in the future.

The text is organized as follows: An overview of the interaction of the solar wind with Venus and Mars is given in the next section, followed by a discussion on the role of solar cycle in the variability of the interaction region extension, ionosphere and escape rate.

2. Solar wind interaction with Mars and Venus. General morphology

Apart from the moon, Venus and Mars are the most visited solar system objects in the history of space exploration. Since the dawn of the space era, many missions have characterized their plasma environments, providing a basis for comparative studies over different periods of solar activity (see Fig. 2).

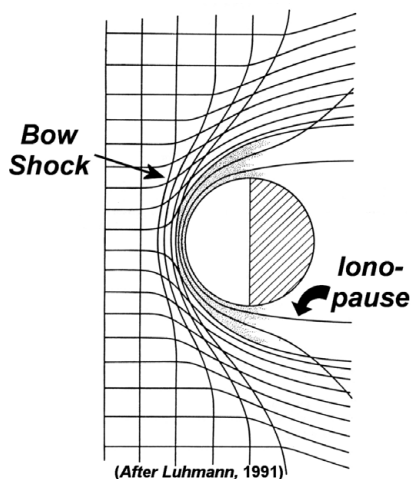


Figure 1. Schematic describing the formation of an induced magnetosphere from the deflection of solar wind stream lines and frozen in magnetic fields (after Luhmann 1991)

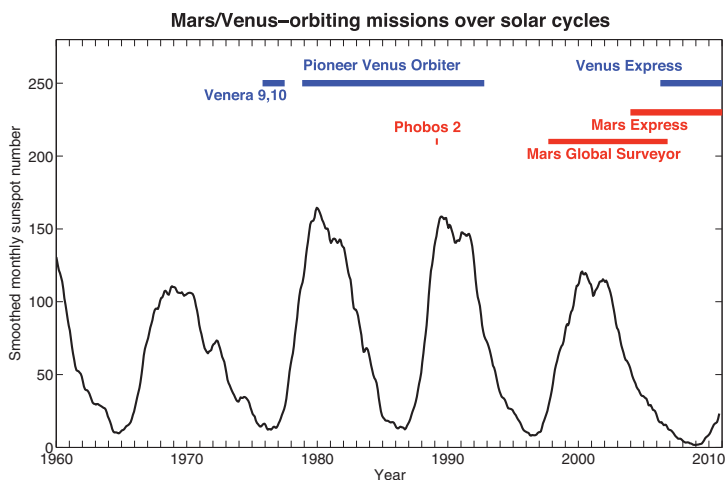


Figure 2. Time coverage of orbiting missions with payload for plasma investigations around Venus (blue, see online version) and Mars (red, see online version) and averaged sunspot number as a function of decimal years since 1960 (source: <http://sidc.oma.be/sunspot-data/>).

2.1. Venus

Current knowledge of the solar wind interaction with Venus comes from the Venera-9 and 10 (e.g., Zeleny and Vaisberg 1985) providing measurements over solar minimum, from the Pioneer Venus Orbiter (PVO) which provided a data set that extended over an entire solar cycle (Russell *et al.* 2006a), and more recently from the Venus Express (VEX) mission, which began its operations in during the last minimum of solar activity.

The plasma environment of Venus has been analyzed using data from the PVO magnetometer OMAG (Russell *et al.* 1980) and plasma analyzers, notably, the Orbiter Retarding Potential Analyzer ORPA (Knudsen *et al.* 1979) because of its higher time resolution. However, compared with VEX's magnetometer MAG (Zhang *et al.* 2006) and the ASPERA-4 plasma analyzer (Barabash *et al.* 2007), PVO instruments had much lower temporal, energy and angular resolution.

Although PVO's temporal coverage includes a whole solar cycle, no direct measurements of the plasma environment during solar minimum were possible due to the high PVO orbital altitude (> 2000 km) at that time. The VEX spacecraft has a constant periapsis altitude of about 250 km and thus can sample this region during solar minimum. Just prior to PVO arrival, the Russian Venera 9 and 10 orbiters (1975, 1976) observed the Venus solar wind interaction, including the bow shock and tail during solar minimum (Verigin *et al.* 1978).

Figure 3 shows VEX ASPERA measurements where the main plasma regions and boundaries around Venus are detected both inbound and outbound from the planet. As the spacecraft approaches Venus, the collisionless bow shock (BS) is clearly defined from the increase in the counts of all measured particles. This corresponds to the increase of the density as the upstream flow is compressed while it becomes subsonic. The heating of the shocked plasma is evident in the outbound leg. Inside the BS, the solar wind plasma becomes increasingly loaded with cold, local plasma and the whole flow continues to decelerate. The IMB (labeled as ICB in the figure) encloses plasma which is mostly cold and of local origin. This is especially noticeable in the oxygen ions. The decrease in all particle counts around the IMB is only apparent. The change in the spacecraft potential prevents electrons with low (a few eVs) energies to be detected. The ionopause (IP) is not clearly observed in the figure, but it is characterized, on the dayside, by the occurrence of local photoelectrons at energies around 20 eV (Coates *et al.* 2011).

These plasma features are correlated with magnetic field signatures. Inside the shock, the magnetosheath is characterized by a high magnetic field variability. At the bottom of the magnetosheath, on the dayside, the magnetic field pileup increases (usually gradually) and a magnetic barrier forms (Zhang *et al.* 1991). The IMB marks the entry into the induced magnetosphere (IM), where piled-up, draped fields coexist with a plasma which is predominantly of planetary origin. The IMB extends to at least 11 planetary radii downstream and encircles the induced tail where planetary plasma escape is concentrated (Saunders and Russell 1986). At the ionopause, the thermal ionospheric pressure is expected to balance the induced magnetosphere's magnetic pressure. When that balance is achieved, the magnetic field is depleted inside the IP. As it will be seen, however, this condition only holds during solar maximum. The lower doses of EUV flux and the increase in periods of high solar wind dynamic pressure during solar minima result in the weakening of the shielding effect of the ionopause and the ionosphere gets magnetized.

2.2. Mars

The in situ exploration of the Martian environment dates back to the very beginning of space era. Following Mariner 4, 6 and 7, Mars 2, 3, and Mariner 9 were probably the first spacecraft to enter the Martian induced magnetosphere (Vaisberg and Bogdanov 1974). At the time of those observations, however, it was still uncertain if Mars possessed an intrinsic magnetic field on its own. This issue was resolved with the arrival of Mars Global Surveyor (MGS). MGS observations revealed that the planet has lacked a global intrinsic magnetic field for at least 4 Gyr (Acuña *et al.* 1998). The absence of a global intrinsic magnetic field at Mars led to the re-interpretation of part of previous plasma measurements. A comprehensive review on the comparison between MGS and Phobos-2 plasma observations within the induced magnetosphere of Mars can be found in Nagy *et al.* 2004. Although the magnetic field and the solar wind electron population were efficiently characterized by MGS' magnetometer and electron reflectometer (MAG/ER) (Acuña *et al.* 1992), MGS did not carry ion instruments.

With an overlap of a few years with MGS, Mars Express (MEX) began its observations in 2003, providing a wide range of particle measurements, without a magnetometer. Solar

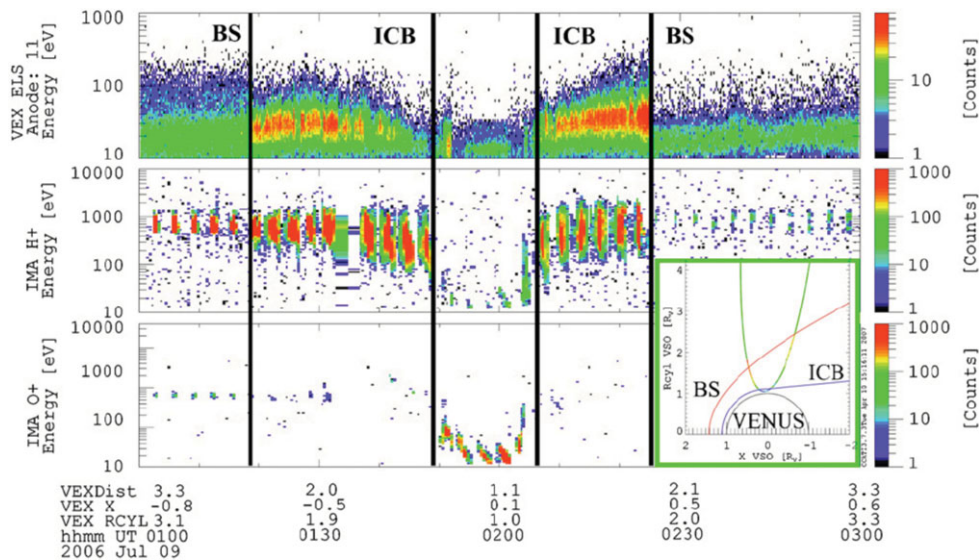


Figure 3. From top to bottom: Electron, H⁺ and O⁺ counts as a function of energy and time measured by VEX ASPERA during an orbit around Venus. The inset in the low right corner depicts the trajectory a planet-centred cylindrical coordinates where the X axis points sunward (from Martinez *et al.* 2008).

wind and planetary particles were measured by the ASPERA-3 instrument, consisting in an electron spectrometer (ELS) and an ion mass analyzer (IMA) (Barabash *et al.* 2006).

Unfortunately, MEX does not carry a magnetometer. Nevertheless, for some orbits, the magnetic field strength and the electron density within the induced magnetosphere can be deduced from the Mars Advanced Radar for Subsurface and Ionospheric Sounding (MARSIS) measurements (Gurnett *et al.* 2005). One capability of the ionospheric sounding mode of MARSIS onboard MEX is the measurement of the local plasma density. Summaries of MEX plasma results can be found in review articles by Franz *et al.* (2006) and Dubinin *et al.* (2006).

Apart from the ULF plasma waves generated by the pick up of exospheric ions, the first perturbation generated by Mars in the supermagnetosonic solar wind flow is the bow shock (Mazelle *et al.* 2004). As for the case of Venus, the Martian bow shock, also decelerates, heats and compresses the solar wind plasma. The end of the turbulent regime of the magnetosheath is marked once again by a well-defined IMB, which precedes the IM and its highly draped magnetic fields and dominating local plasma. The IMB extends out into the downstream sector where it becomes the outer boundary of the magnetic tail. The IMB has several subregions. On the dayside, the region below the IMB and above the ionospheric boundary is referred to as the magnetic pileup region (MPR). At low magnetic latitudes, the interplanetary magnetic field (IMF) within the MPR is connected to tail lobe fields. The ionospheric boundary marks the lower end of the MPR on the dayside. Usually referred to it as photoelectron boundary (PEB), this boundary is usually associated with the upper limit of the collisional ionosphere. The PEB and to a lesser extent the IMB locations are influenced by the magnetic fields from the crustal sources. In the downstream sector, a tail plasma sheet separating both tail lobes is observed. The plasma structure of the plasma sheet close to the planet is still under scrutiny with a strong effect of the crustal magnetic sources in the nightside.

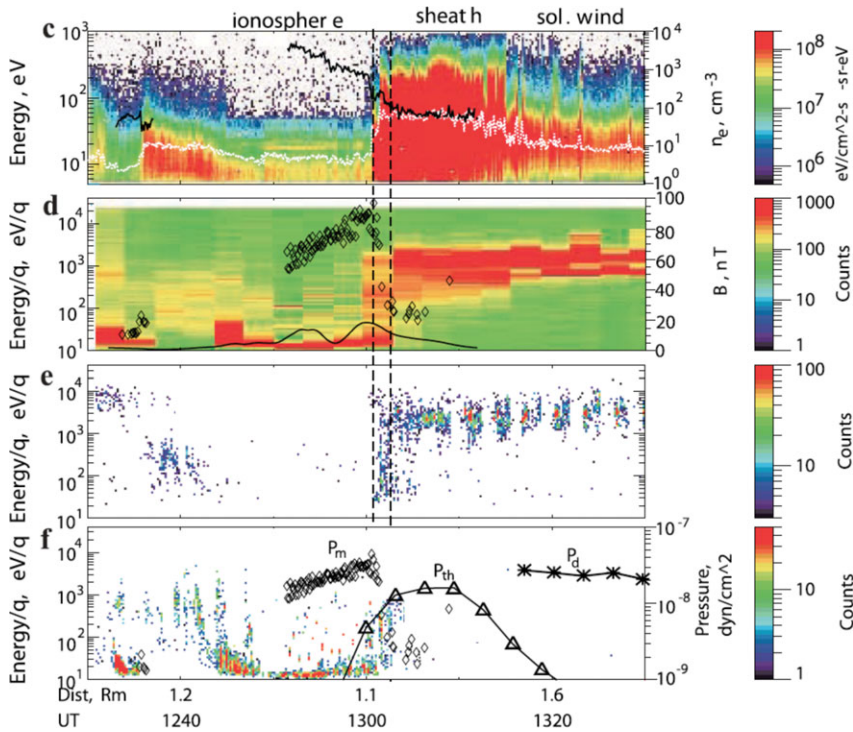


Figure 4. MEX ASPERA/MARSIS measurements (Dubinin *et al.* 2008). The dashed curve corresponds to the position of the IMB. Energy-time spectrograms of the (c) electrons with the imposed curves of pseudo electron density from ASPERA (white) and total electron density from MARSIS (black) and (d) all ion species, (e) He⁺⁺, and (f) heavy ($m/q > 16$) ions. Imposed curves are: the magnetic field value from the MARSIS observations (diamonds) and Cain *et al.* (2003) crustal field model (solid) (d), the magnetic pressure P_m (diamonds), the thermal proton pressure P_{th} (triangles), and the solar wind ram pressure P_d (asterisks).

Figure 4 shows different plasma boundaries and regions around Mars as seen by ASPERA and MARSIS during the outbound leg of a MEX orbit. Based on similar signatures described for Venus, the IMB and BS are clearly detected around 13:00 and 13:16. In particular, magnetic field strength calculated from the MARSIS ionospheric sounding experiment clearly shows the increase in the pileup at the IMB as an increase of the magnetic pressure P_m .

3. Solar influence

3.1. Venus

Venus' induced magnetosphere has proven to be strongly dependent on the Solar cycle phase. Such an effect is probably linked to the EUV flux variability which influences the extension of the ionosphere and the ion pick up rates.

Alexander and Russell (1985), Russell *et al.* (1988) and Zhang *et al.* (1990) investigated the Venus bow shock location based on nearly 2000 PVO boundary crossings. These works concluded that the shock location depends on the solar cycle and solar EUV flux, the upstream solar wind parameters, and the orientation of the IMF (see also Phillips and McComas 1991).

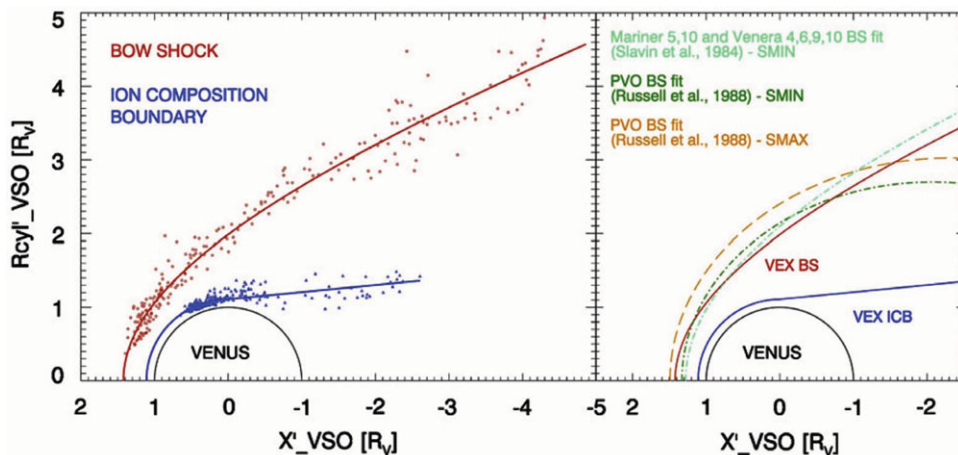


Figure 5. BS (red, see online version) and IMB (blue, see online version) crossings by VEX in aberrated cylindrical VSO coordinates where the X-axis points towards the Sun taking into account the planet's orbital speed (Martinez, *et al.* 2008)

Figure 5a shows Martinez *et al.* (2008) VEX BS and IMB fits and in Figure 5b a comparison with other shock models based on other data sets at solar minimum. The VEX BS fit is in good agreement with the model of Slavin *et al.* (1984) based on Mariner 5,10 and Venera 4, 6, 9, 10 observations.

During solar minimum, a comparison between the BS position and solar EUV flux (F50 index: 0.1 - 50 nm integrated photons $\text{cm}^{-2} \text{s}^{-1}$ and shifted to Venus) derived from SOHO SEM observations shows no apparent dependence (Martinez *et al.* 2008). This is probably due to the fact that the EUV flux variation is small over the period of observation.

As for the Venusian IMB, VEX provided a fit (Figure 5a) corresponding to the location of the boundary during solar minimum. Unfortunately, there is no comparison with similar fit obtained during solar maximum yet. This is partly due to the low time resolution of the PVO ion plasma measurements.

The ionopause has been shown to be strongly influenced by the solar cycle. During solar minimum, the pressure balance defining the boundary is achieved in general at lower altitudes in comparison with solar maximum (Russell and Vaisberg 1983). Also, the ionosphere is more magnetized during solar minimum, as the thermal pressure in the ionosphere is not enough to withstand the magnetic pressure in the barrier. Also, the ionopause altitude seems to control the ionospheric O^+ flow into the nightside, probably affecting the escape. Figure 6 shows the flow pattern of O^+ ions during solar maximum (Miller and Whitten 1991). During solar minimum, however, this circuit disappears, leading to the idea that the lower location of the pressure balance boundary might disrupt ionospheric flow.

During the VEX era, ASPERA measurements across the magnetotail of Venus have confirmed the fact that planetary ions (H^+ and O^+) escape from Venus due to the solar wind interaction (Barabash *et al.* 2007). In particular, escape rates have been shown to increase by a factor of 2 during the passage of CIR and ICMEs (Edberg *et al.* 2011). This indicates the importance of disturbed solar wind periods in the atmospheric escape at unmagnetized objects.

Figure 5 shows antisunward fluxes of planetary O^+ ions during the passage of CIRs/ICMEs (top panel), during periods of 'quiet' solar wind (middle panel) and the ratio

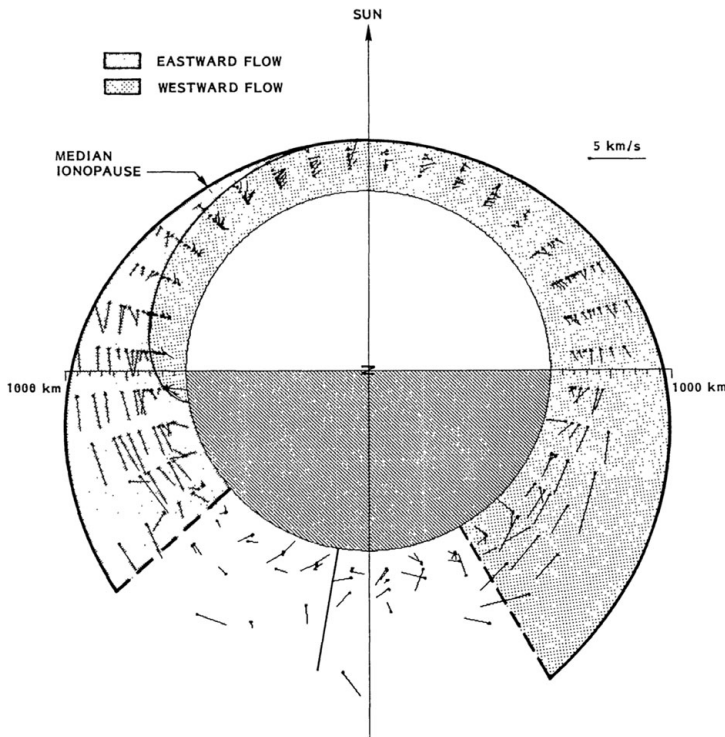


Figure 6. Velocity vectors of O^+ ions within the Venusian ionosphere from PVO observations (Miller and Whitten 1991). The shaded area identifies the westward flow, whereas the white region encloses the area where the flow vectors point eastwards.

between disturbed solar wind times and quiet times in each bin (bottom panel). As shown in the figures (in particular in the bottom panel) the fluxes, concentrated inside the IMB are enhanced during the disturbed periods. Unfortunately, this study has not been done for solar maximum conditions.

McEnulty *et al.* (2010) studied 17 ICME events and demonstrated that the energy (but not the flux) of pickup ions around Venus increases whenever the planet is impacted by an ICME. Earlier, Luhmann *et al.* (2007) showed that atmospheric escape could increase by a factor of 100 during ICMEs, as measured by the PVO spacecraft.

However, case studies of the influence of ICMEs have left ambiguous results, since in 3 out of 4 cases studied by Luhmann *et al.* (2008), the escape rate was not observed to increase. Futaana *et al.* (2008) showed that another single large ICME associated with simultaneous increase in solar energetic particle flux increased the atmospheric escape rate at both Venus and Mars, by a factor of $\approx 5 - 10$. It should be mentioned that McEnulty *et al.* (2010) and Luhmann *et al.* (2007) looked at the escape of high energy ions only while Futaana *et al.* (2008) included all ions.

3.2. Mars

The shape and location of the Martian BS and IMB have been studied in the past by e.g. Slavin and Holzer (1981), Vignes *et al.* (2000), Bertucci *et al.* (2005), Trotignon *et al.* (2006) and Edberg *et al.* (2008). During the Phobos 2 mission the number of bow shock and IMB crossings were 127 and 41, whereas during the MGS mission, 573 (Trotignon *et al.* 2006) and 1149 (Bertucci *et al.* 2005), respectively. In the data set of MEX/ASPERA-3 from 2004 until 2008 have 5014 IMB crossings and 3277 BS crossings

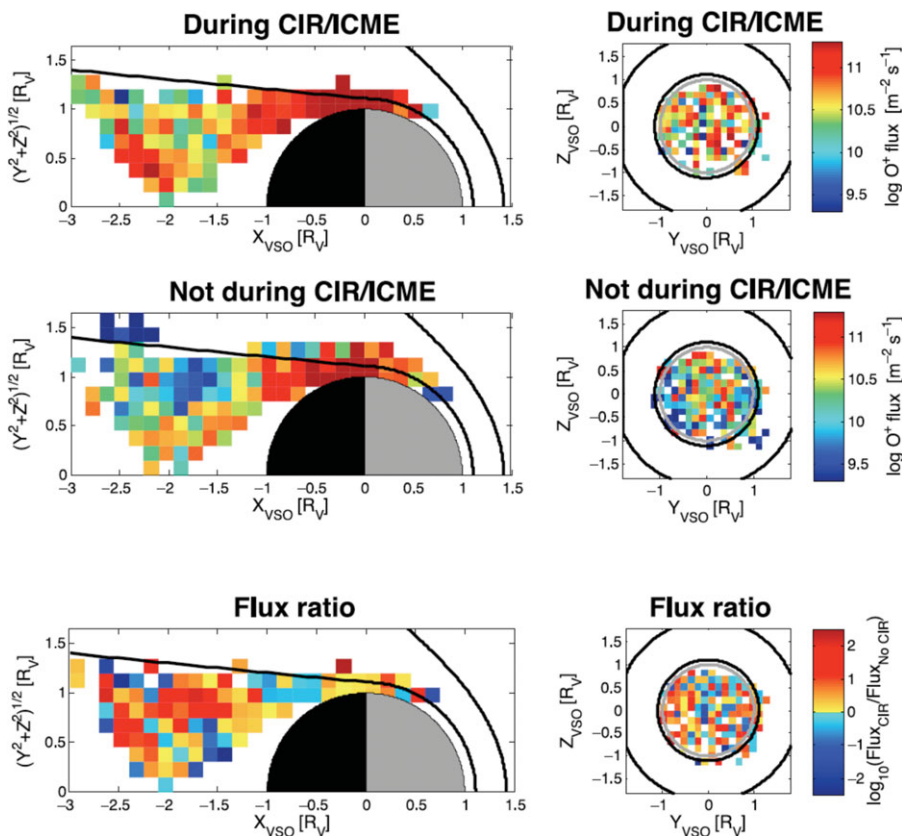


Figure 7. Antisunward fluxes of planetary O^+ ions as measured (top) during the impact of CIRs/ICMEs and (middle) during the time of quiet solar wind as well as (bottom) the flux ratio between disturbed solar wind times and quiet times in each bin (Edberg *et al.* 2011). The data is shown (left) in cylindrical VSO coordinates as well as (right) in the VSO $y-z$ plane for $-3 \text{ RV} < x < -1 \text{ RV}$. Each bin is $0.15 \times 0.15 \text{ RV}$ large and contains at least 4 measurement points. The black lines indicate the average locations of the BS and the IMB from Martinecz *et al.* (2008) and the grey circles indicate the limb of the planet.

been identified (Edberg *et al.* 2009). The number of crossings during the overlapping mission time between MGS and MEX (Feb 2004 - Nov 2006) is 2500 and 1840, respectively.

Figure 8 shows the conic section fits of the BS and IMB from Phobos 2 (solar maximum) and MGS (solar minimum) (Vignes *et al.* 2000). Contrary to the behaviour observed at Venus, there is not appreciable difference in the location of these boundaries with solar cycle.

However, high variability in the location of these boundaries is observed for shorter timescales. The factors that have been studied for possible effects on the location of these boundaries include the IMF direction (Vignes *et al.* 2000, Brain *et al.* 2005), the crustal magnetic fields (Crider *et al.* 2002, Dubinin *et al.* 2006, Fränz *et al.* 2006, Edberg *et al.* 2008, Edberg *et al.* 2009), the solar wind dynamic pressure (Crider *et al.* 2003, Brain *et al.* 2005, Edberg *et al.* 2009), and the magnetosonic Mach number (Edberg *et al.* 2010). In some of these studies, proxies derived from extrapolated in situ measurements around 1 AU have been used (e.g. Edberg *et al.* 2010). Of these studies, it is worth mentioning that of the influence of the crustal magnetic fields (Acuña *et al.* 1999) on boundary locations (Crider *et al.* 2002, Brain *et al.* 2005, Fränz *et al.* 2006, Edberg *et al.* 2008, Edberg *et al.*

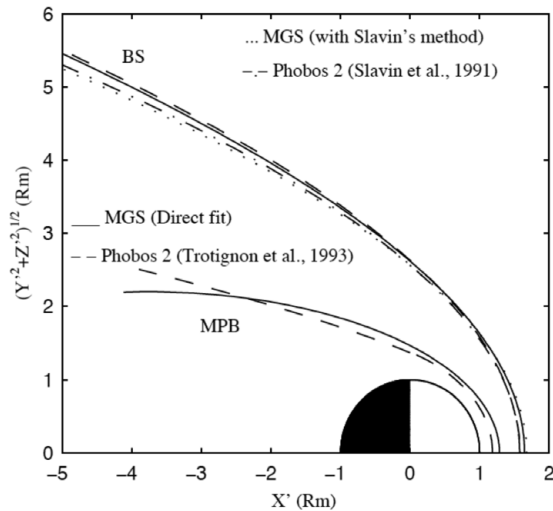


Figure 8. Conic section fits of the Martian BS and IMB obtained from Phobos-2 and MGS spacecraft during Solar maximum and minimum respectively.

2009). All these studies conclude that crustal fields do affect the altitude of the IMB, but that there is ambiguous evidence of the influence on the shock. In spite of the effect on the IMB, however, the role of crustal sources in the rate of plasma escape is thought to be negligible (Dubinin *et al.* 2006).

On the other hand, a clear influence of the solar cycle on the exospheric structure is predicted by current models of exosphere. In particular, Modolo *et al.* (2005) made use of a Chamberlain model of the O and H exospheres for Mars for their global kinetic simulations of the environment of Mars noting an inflation of the exospheres during solar maximum (Figure 9).

Modolo *et al.* (2005) also showed that the oxygen escape, as well as the hydrogen escape, is strongly dependent on the solar EUV flux. Whatever the solar EUV flux is, however, between 85 and 90% of the escaping proton flux comes from charge exchange. The escape flux of H^+ ions is approximately four times higher during solar minimum than during solar maximum, due to the inflation of the neutral hydrogen corona at solar minimum. On the other hand, photoionization is the main process which contributes to the escape of O^+ ions, which maximizes at solar maximum with the extension of oxygen corona.

As for the influence of solar wind energetic transient phenomena, Edberg *et al.* (2010) found that the atmospheric escape rate at Mars is not constant but rather increases by a factor of ~ 2.5 on average during the pass of CIRs and ICMEs. Dubinin *et al.* (2009) similarly showed that a single large CIR that impacted on Mars increased the scavenging of the ionosphere, with the escape rate again being estimated to increase by a factor of ~ 10 .

4. Summary

In this work, we described how induced magnetospheres are the result of the direct interaction of the atmospheres of unmagnetized objects with the solar wind and how they are more prone to atmospheric evolution than magnetized planets. In particular, the cases of Venus and Mars have been analyzed, by discussing the influence of the solar

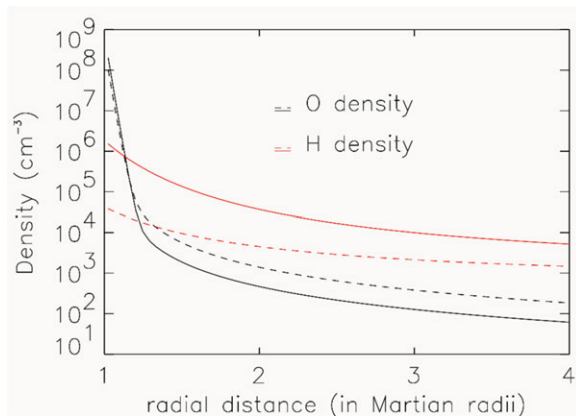


Figure 9. Chamberlain Hydrogen and oxygen vertical density profiles at solar minimum (solid lines) and solar maximum (dashed lines) (Modolo *et al.* 2005)

cycle and solar wind variability with the structure of their induced magnetospheres and resulting escape rate.

Plasma measurements obtained around Venus suggest that plasma regions and escape seem to be strongly influenced by solar cycle. However, most of the studies involving high time resolution plasma measurements are available only for solar minimum. At Mars, on the other hand, the epochal coverage by Phobos-2 and MGS show that plasma boundaries would not be dependent on the solar cycle phase, although simulations suggest that escape is as a result of the change in the EUV flux. Current escape rates of the order of 1025 part/s are estimated (Edberg *et al.* 2011 and references therein) but estimates may double and even increase by an order of magnitude during stormy space weather.

We expect to find similar scenarios at other planetary systems but it is still difficult to assess those interactions in the absence of in situ measurements. Techniques involving remote sensing will have to be used in order to look for observables obtained from models built and validated from local in situ observations.

References

- Acuña, M. H. *et al.* 1992, *Jour. of Geophys. Res.*, 97E5, 7799
 Acuña, M. H. *et al.* 1998, *Science*, 279, 1676
 Acuña, M. H., *et al.* 1999, *Science*, 284, 790
 Alexander, C. J. & Russell, C. T. 1985, *Geophys. Res. Lett.*, 12(6), 369
 Barabash, S. *et al.* 2006, *Space Sci. Rev.*, 126, 113
 Bertucci, C. *et al.* 2003, *Geophys. Res. Lett.*, 30(2), 1099
 Bertucci, C. *et al.* 2003, *Geophys. Res. Lett.*, 30(17), 1876
 Bertucci, C. *et al.* 2005, *Jour. of Atmos. and Solar-Terres. Phys.*, 67(17-18), 1797
 Bertucci, C. *et al.* 2011, *Space Sci. Rev.*, 162(1-4), 113
 Brain, D. A. *et al.* 2005, *Geophys. Res. Lett.*, 32, 1820
 Cain, J. C. *et al.* 2003, *Jour. of Geophys. Res.*, 108(E2), 5008
 Coates, A. J. *et al.* 2011, *Planetary and Space Science*, 59(10), 1019
 Crider, D. H. *et al.* 2002, *Geophys. Res. Lett.*, 29, 1170
 Crider, D. H. *et al.* 2003, *Jour. of Geophys. Res.*, 108(A12), 12
 Dubinin, E. *et al.* 2006, *Space Sci. Rev.*, 126(1-4), 209
 Dubinin, E. *et al.* 2008, *Geophys. Res. Lett.*, 35, 11103
 Dubinin, E. *et al.* 2009, *Geophys. Res. Lett.*, 36, 1105
 Dubinin, E. *et al.* 2011, *Space Sci. Rev.*, 162(1-4), 173

- Edberg, N. J. T. *et al.* 2008, *Jour. of Geophys. Res.*, 113(A8), 206
- Edberg, N. J. T. *et al.* 2009, *Ann. Geophys.*, 27(9), 3537
- Edberg, N. J. T. *et al.* 2010, *Jour. of Geophys. Res.*, 115(A7), 203
- Edberg, N. J. T. *et al.* 2011, *Jour. of Geophys. Res.*, 116(A9), 308
- Fedorov, A. *et al.* 2008, *Planetary and Space Science*, 56, 812
- Fränz, M. *et al.* 2006, *Space Sci. Rev.*, 126(1-4), 165
- Futaana, Y. *et al.* 2008, *Planetary and Space Science*, 56(6), 873
- Gurnett, D. A. *et al.* 2005, *Science*, 310, 1929
- Knudsen *et al.* 1979, *Space Sci. Instrum.*, 4, 351
- Luhmann, J. G. 1991, *Rev. Geophys.*, 29, 965
- Luhmann, J. G. *et al.* 2007, *Jour. of Geophys. Res.*, 112(A4), 10
- Luhmann, J. G. *et al.* 2008, *Jour. of Geophys. Res.*, 113(A5), 2
- Martinez, C. *et al.* 2008, *Planetary and Space Science*, 56(6), 780
- Mazelle, C. *et al.* 2004, *Space Sci. Rev.*, 111(1-4), 115
- McEnulty, T. R. 2010, *Planetary and Space Science*, 58(14-15), 1784
- Miller, K. L. & Whitten, R. C. 1991, *Space Sci. Rev.*, 55, 165
- Modolo, G. M. *et al.* 2005, *Ann. Geophys.*, 23, 433
- Nagy, A. F. *et al.* 2004, *Space Sci. Rev.*, 111, 33
- Ness, N. F. *et al.* 1982, *Jour. of Geophys. Res.*, 87(A3), 1369
- Phillips, J. L. & McComas, D. J. 1991, *Space Sci. Rev.*, 55, 1
- Russell, C. T. *et al.* 1980, *IEEE trans. Geosci. Electron.*, GE-18, 32
- Russell, C. T. & Vaisberg, O. 1983, *Venus, University of Arizona Press, edited by D.M. Hunton, L. Colin, T.M. Donahue, V.I. Moroz*, 873
- Russell, C. T. *et al.* 1988, *Jour. of Geophys. Res.*, 93, 5461
- Russell, C. T. *et al.* 2006, *Planetary and Space Science*, 54, 1482
- Saunders, M. A. & Russell, C. T. 1986, *Jour. of Geophys. Res.*, 91(A5), 589
- Slavin, J. A. & Holzer, R. E. 1981, *Jour. of Geophys. Res.*, 86(A11), 401
- Slavin, J. A. *et al.* 1984, *Jour. of Geophys. Res.*, 89(A5), 2708
- Szego, K., *et al.* 2000, *Space Sci. Rev.*, 94(3-4), 429
- Trotignon, J. G. *et al.* 2006, *Planetary and Space Science*, 54, 357
- Vaisberg, O. L. & Bogdanov, A. V. 1974, *Cosmic Research*, 12, 253
- Verigin, M. I. *et al.* 1978, *Jour. of Geophys. Res.*, 83(A8), 3721
- Vignes, D. *et al.* 2000, *Geophys. Res. Lett.*, 27(1), 49
- Vignes, D. *et al.* 2002, *Geophys. Res. Lett.*, 29(9), 1329
- Zelenyi, L. M. & Vaisberg, O. L. 1985, *Advances of Space Plasma Physics, ed. Buti, World Scientific*, 59
- Zhang, T.-L. *et al.* 1990, *Jour. of Geophys. Res.*, 95(A14), 961
- Zhang, T.-L. *et al.* 1991, *Jour. of Geophys. Res.*, 96(A11), 153
- Zhang, T.-L. *et al.* 1991, *Planetary and Space Science*, 54, 1336

Discussion

MARK GIAMPAPA: This is a source of erosion of planetary magnetospheres. Can you extrapolate this to the past, to times of high solar activity?

CÉSAR BERTUCCI: Yes, there are a few works that have addressed the cumulative escape due to solar wind interaction since the Sun reached ZAMS. I suggest you to read the review article by Lammer *et al.* (2006, *Space Sci. Rev.* 122, 189). However, in my opinion much needs to be further understood before extrapolating current escape rates. Thanks for your interest.